Proceedings of the
46th IEEE Conference on Decision and Control
New Orleans, LA, USA, Dec. 12-14, 2007

POD-Based Predictive Controller with Temperature Constraints for a Tubular Reactor

Oscar Mauricio Agudelo, Jairo José Espinosa, *Senior Member, IEEE,*
and Bart De Moor, *Fellow Member, IEEE*

***Abstract*— In this paper the control of a non-isothermal tubular reactor is addressed using Proper Orthogonal Decomposition (POD) and predictive control techniques. The proposed control system has the goal of keeping the operation of the reactor around a given operating condition in spite of the disturbances in the feeding flow. Additionally the controller has to avoid that the temperature inside the reactor be larger than a given value in order to prevent undesirable side reactions. The proposed control system handles this constraint as a soft-constraint and it uses a slack variable approach with l_∞-norm and time-dependent weights to handle the infeasibilities that can emerge. The MPC controller is based on a model derived by means of the POD technique, which reduces the high dimensionality of the discretized system used to approximate the Partial Differential Equations (PDEs) that model the reactor. The simulation results show that the predictive controller presented a good behavior and that it dealt with the temperature constraint quite well.**

I. INTRODUCTION

Tubular reactors are typically modeled by nonlinear Partial differential Equations (PDEs) that are derived from mass and energy balance principles. For the design of the control systems usually such PDEs are approximated by a large number of Ordinary differential equations (ODEs). Afterwards, given the high-dimensionality of the resulting models, reduced order models are derived to make possible the design of the controllers. In this paper such reduced order models are found by means of Proper Orthogonal Decomposition (POD). The advantage of applying this technique is the incorporation of simulation or experimental data as well as the existing physical relationships from the original model [6].

In [1], the authors propose a POD-based MPC control scheme for controlling the temperature and concentration profiles of a non-isothermal tubular reactor. Such MPC control system has the goal of rejecting the disturbances that affect the tubular reactor, that is the changes in the temperature and concentration of the feeding flow. The formulation of the MPC presented in [1] is in terms of the POD coefficients, which have no physical meaning. This makes the tuning of the controller little intuitive and the definition of the control goals little flexible; for example, we can not give more weight to the reduction of the concentration deviations at the reactor outlet than to the reduction of the temperature deviations, or viceversa. One important constraint of the system is that the temperature inside the reactor must be smaller than a given value in order to avoid the formation of side products. This constraint is not incorporated in the MPC formulation presented in [1].

In this paper a new POD-based MPC control scheme is proposed. In this scheme, the MPC formulation is in terms of physical variables (the temperature of some selected points and the concentration at the reactor outlet), and incorporates the temperature constraint of the reactor. The MPC uses a slack variables approach with l_∞-norm and time-dependent weights for handling the infeasibilities that can emerge [7].

The paper is organized as follows. In Section II a description of the reactor is presented. Section III shows the derivation of the reduced order model of the reactor by means of the POD technique. In Section IV the design of the MPC controller with temperature constraints is described, and the simulation results are presented. Finally Section V summarizes the main conclusions.

II. TUBULAR REACTOR

The system to be controlled is a non-isothermal tubular reactor where a single, first order, irreversible, exothermic reaction takes place ($A \rightarrow B$). The reactor is surrounded by 3 cooling/heating jackets as it is shown in Figure 1. The temperature of the jackets fluids ($T_{\mathrm{J}1}, T_{\mathrm{J}2}$ and $T_{\mathrm{J}3}$) can be manipulated independently in order to control the reactor profiles. In this study the heat transfer effects between the jackets fluids and the reactor wall are neglected, and the diffusion and dispersion phenomena are not taken into account (plug-flow behavior). Under the previous assumptions, the mathematical model of the tubular chemical reactor consists of the following coupled non-linear PDEs:

$$\begin{aligned} \frac{\partial C}{\partial t} &= -v\frac{\partial C}{\partial z} - k_0 C e^{-\frac{E}{RT}} \\ \frac{\partial T}{\partial t} &= -v\frac{\partial T}{\partial z} + G_{\mathrm{r}} C e^{-\frac{E}{RT}} + H_{\mathrm{r}}(T_{\mathrm{w}} - T) \\ G_{\mathrm{r}} &= \frac{-\Delta H k_0}{\rho C_{\mathrm{p}}}, \quad H_{\mathrm{r}} = \frac{4h}{d\rho C_{\mathrm{p}}} \end{aligned} \tag{1}$$

with the following boundary conditions:

$$C = C_{\mathrm{in}} \text{ at } z = 0 \text{ and } T = T_{\mathrm{in}} \text{ at } z = 0$$

O. M. Agudelo is with the Department of Electrical Engineering (ESAT), Research Group SCD-SISTA, Katholieke Universiteit Leuven, Kasteelpark Arenberg 10, B-3001 Heverlee (Leuven), Belgium. He is also with the Department of Automation and Electronics, Universidad Autnoma de Occidente, Calle 25 No 115-85, Cali, Colombia. mauricio.agudelo@esat.kuleuven.be

J. J. Espinosa is with the Facultad de Minas, Universidad Nacional de Colombia, Carrera 80 No. 65-223, Medellin, Colombia. jairo.espinosa@ieee.org

B. De Moor is with the Department of Electrical Engineering (ESAT), Research Group SCD, Katholieke Universiteit Leuven, Kasteelpark Arenberg 10, B-3001 Heverlee (Leuven), Belgium. bart.demoor@esat.kuleuven.be

1-4244-1498-9/07/$25.00 ©2007 IEEE.

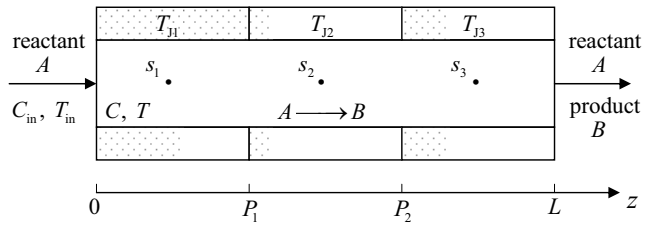

Fig. 1. Tubular Chemical Reactor with 3 cooling/heating jackets.

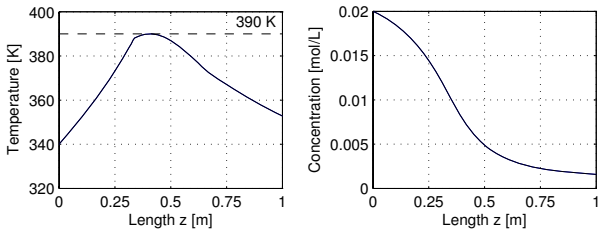

Fig. 2. Steady-State Concentration and Temperature profiles (Operating Profiles) when $T_{\mathrm{J1}} = 374.6$ K, $T_{\mathrm{J2}} = 310.1$ K and $T_{\mathrm{J3}} = 325.2$ K.

where $C(z,t)$ is the reactant concentration in [mol/L], $T(z,t)$ is the reactant temperature in [K], v is the fluid superficial velocity in [m/s], $(-\Delta H)$ is the heat of the reaction in [cal/mol], ρ and C_{p} are the density in [Kg/L] and the specific heat in [cal/Kg/K] of the mix respectively, k_0 is the kinetic constant in [1/s], E is the activation energy in [cal/mol], R is the ideal gas constant in [cal/mol/K], h is the heat transfer coefficient in [cal/s/m^2/K], d is the reactor diameter in [m], L is the reactor length in [m], C_{in} and T_{in} are the concentration in [mol/L] and the temperature in [K] of the feeding flow, z is the axial coordinate in [m], t is the time in [s] and $T_{\mathrm{w}}(z,t)$ is the reactor wall temperature in [K] defined as follows (see Figure 1),

$$T_{\mathrm{w}} = \begin{cases} T_{\mathrm{J1}}, & 0 \le z < P_1 \\ T_{\mathrm{J2}}, & P_1 \le z < P_2 \\ T_{\mathrm{J3}}, & P_2 \le z \le L. \end{cases}$$

The parameters of the reactor model are taken from [2] which were inspired by the values given in [3]. These values are: $v = 0.1$ m·s^{-1}, $L = 1$ m, $k_0 = 10^6$·s^{-1}, $E = 11250$ cal·mol^{-1}, $R = 1.986$ cal·mol^{-1}·K^{-1}, $C_{\mathrm{in}} = 0.02$ mol·L^{-1}, $T_{\mathrm{in}} = 340$ K, $G_{\mathrm{r}} = 4.25 \cdot 10^9$ L·K·mol^{-1}·s^{-1}, and $H_{\mathrm{r}} = 0.2$ s^{-1}.

The temperature of the jacket sections T_{J1}, T_{J2} and T_{J3} must be between 280 K and 400 K (input constraints). In addition, the temperature inside the reactor must be smaller than 400 K (output constraint) in order to avoid the formation of side products. The kind of disturbances that affects the reactor are the variations in the temperature and concentration of the feeding flow. Typically such variations are ± 10 K for temperature and $\pm 5\%$ of the nominal value for the concentration. In this system only the temperature of the feeding flow is measured directly. In addition, the reactor has a temperature sensor at the output and 3 temperature sensors (s_1, s_2 and s_3) distributed in its interior as it is shown in Figure 1.

A. Operating Profiles

The operating profiles of the reactor are the optimal operating profiles found in [1] by means of an optimization algorithm (a kind of SQP), which miminizes a cost function subject to the discrete steady-state equations (the reactor was divided into 300 sections) of the tubular reactor described by (1) and the input and output constrains of the system. These profiles are shown in Figure 2 together with the corresponding jackets temperatures. The concentration at the reactor output is $1.5737 \cdot 10^{-3}$ mol/L which is 12.7 times smaller than the concentration of the feeding flow (0.02 mol/L). In the algorithm, the maximum allowed temperature inside the reactor (output constraint) was set 10 degrees smaller than the real limit (400 K) in order to give to the feedback controller enough room of maneuverability. From Figure 2 it is clear that the maximum peak of the temperature profile is 390 K, which satisfies the temperature constraint imposed in the algorithm.

B. Linear Model

The linear model of the tubular reactor was obtained by linearizing (1) around the jackets temperatures and the operating profiles presented in Figure 2 by using the Taylor series. Afterwards in order to reduce the infinite dimensionality of the resulting linear PDEs, the partial derivatives with respect to space were replaced by backward difference approximations leading to the following system of ODEs:

$$\dot{\mathbf{x}}(t) = \mathbf{A}\mathbf{x}(t) + \mathbf{B}\mathbf{u}(t) + \mathbf{F}\mathbf{d}(t) \tag{2}$$

$$\mathbf{x}(t) = (\bar{C}_1^{\Delta}, \bar{C}_2^{\Delta}, ..., \bar{C}_N^{\Delta}, \bar{T}_1^{\Delta}, \bar{T}_2^{\Delta}, ..., \bar{T}_N^{\Delta})^T$$

$$\mathbf{d}(t) = (\bar{C}_{\mathrm{in}}^{\Delta}, \bar{T}_{\mathrm{in}}^{\Delta})^T, \ \mathbf{u}(t) = (\bar{T}_{\mathrm{J1}}^{\Delta}, \bar{T}_{\mathrm{J2}}^{\Delta}, \bar{T}_{\mathrm{J3}}^{\Delta})^T$$

where C_i^*, T_i^* are the steady state concentration and temperature of the ith section, C_{in}^* and T_{in}^*, are the steady state concentration and temperature of the feeding flow, T_{J1}^*, T_{J2}^*, T_{J3}^* are the steady state jacket temperatures, T_{f} and C_{f} are normalization factors, $\bar{C}_i^{\Delta} = (C_i - C_i^*)/C_{\mathrm{f}}$, $\bar{T}_i^{\Delta} = (T_i - T_i^*)/T_{\mathrm{f}}$ are the normalized deviations from steady state of the concentration and temperature of the ith section, $\bar{C}_{\mathrm{in}}^{\Delta} = (C_{\mathrm{in}} - C_{\mathrm{in}}^*)/C_{\mathrm{f}}$ and $\bar{T}_{\mathrm{in}}^{\Delta} = (T_{\mathrm{in}} - T_{\mathrm{in}}^*)/T_{\mathrm{f}}$ are the normalized deviations from steady state of the concentration and temperature of the feeding flow, $\bar{T}_{\mathrm{J1}}^{\Delta} = (T_{\mathrm{J1}} - T_{\mathrm{J1}}^*)/T_{\mathrm{f}}$, $\bar{T}_{\mathrm{J2}}^{\Delta} = (T_{\mathrm{J2}} - T_{\mathrm{J2}}^*)/T_{\mathrm{f}}$ and $\bar{T}_{\mathrm{J3}}^{\Delta} = (T_{\mathrm{J3}} - T_{\mathrm{J3}}^*)/T_{\mathrm{f}}$ are the normalized deviations of the jacket temperatures, N is the number of sections in which the reactor is divided, $\mathbf{A}$, $\mathbf{B}$ and $\mathbf{F}$ are the matrices describing the system, $\mathbf{x}(t)$ is the state vector, $\mathbf{u}(t)$ is the vector of the inputs, and $\mathbf{d}(t)$ is the vector of the disturbances.

The spatial domain was divided into $N = 300$ sections which means that (2) has 600 states. Since it is not easy to design a control system that can deal with 600 states, a reduced order model has to be found. In this paper such reduced order model is derived by means of the POD technique.

III. Model reduction by means of POD

In proper orthogonal decomposition, we postulate that $\mathbf{x}(t) \in \Re^{2N}$ can be expanded as a sum of orthonormal basis vectors:

$$\mathbf{x}(t) = \sum_{j=1}^{2N} a_j(t)\boldsymbol{\varphi}_j \tag{3}$$

where $\boldsymbol{\varphi}_j \in \Re^{2N}\ \forall j = 1, \ldots, 2N$ is a set of orthonormal basis vectors (POD basis vectors o POD basis functions) in the discretized spatial domain, and $a_j(t) \in \Re\ \forall j = 1, \ldots, 2N$ are the time varying coefficients or POD coefficients associated to each basis vector. These POD basis vectors are ordered according to their relevance to $\mathbf{x}(t)$.

The main dynamics of the system can be represented using the first n most relevant basis vectors, since $\boldsymbol{\varphi}_j\ \forall j = 1, \ldots, n$ condensates the main spatial correlations. An nth order approximation of (3) is then given by means of the truncated sequence

$$\mathbf{x}_n(t) = \sum_{j=1}^{n} a_j(t)\boldsymbol{\varphi}_j, \quad n \ll 2N. \tag{4}$$

An approximate (reduced order) model of $\mathbf{x}(t)$ can be derived by building a model for the first n time varying coefficients. "This is the essence of model reduction by POD".

The POD basis vectors are determined from simulation or experimental data (Snapshot matrix) of the process. The dynamic model for the first n time varying coefficients can be found by means of the Galerkin projection [4] or using subspace identification techniques [5].

The derivation of a reduced order model of (2) was done in 5 steps. These steps are explained in detail in [1]. In the following subsections the first 4 steps are described briefly. The fifth step which corresponds to the validation of the reduced order model is not presented in this paper for space reasons.

A. Generation of the snapshot Matrix

A snapshot matrix $\mathbf{X}_{\text{snap}} \in \Re^{600\times 1500}$ was constructed from the system response when independent step changes were made in the input ($\mathbf{u}(t)$) and perturbation ($\mathbf{d}(t)$) signals of the linear model (2).

$$\mathbf{X}_{\text{snap}} = (\mathbf{x}(t = \Delta t), \ldots, \mathbf{x}(t = 1500\Delta t)) \tag{5}$$

Along the simulations, 1500 samples were collected using a sampling time (Δt) of 0.05 sec.

B. Derivation of the POD basis vectors

They were derived by calculating the singular value decomposition (SVD) of $\mathbf{X}_{\text{snap}}$,

$$\mathbf{X}_{\text{snap}} = \boldsymbol{\Phi}\boldsymbol{\Sigma}\boldsymbol{\Psi}^T$$

where $\boldsymbol{\Phi} \in \Re^{600\times 600}$ and $\boldsymbol{\Psi} \in \Re^{1500\times 1500}$ are unitary matrices, and $\boldsymbol{\Sigma} \in \Re^{600\times 1500}$ is a matrix which contains the singular values of $\mathbf{X}_{\text{snap}}$ in a decreasing order on its main diagonal. The columns of Φ are the POD basis vectors.

$$\boldsymbol{\Phi} \in \Re^{600\times 600} = (\boldsymbol{\varphi}_1, \boldsymbol{\varphi}_2, \ldots \boldsymbol{\varphi}_{600})$$

C. Selection of the most relevant POD basis vectors

It was done by checking the singular values of $\mathbf{X}_{\text{snap}}$. The larger the singular value the more relevant the basis vector is. The first 20 basis vectors associated to the first 20 largest singular values were selected. The 20th order approximation of $\mathbf{x}(t)$ is given by

$$\mathbf{x}_{20}(t) = \sum_{j=1}^{20} a_j(t)\boldsymbol{\varphi}_j = \boldsymbol{\Phi}_n\mathbf{a}(t) \tag{6}$$

where $\boldsymbol{\Phi}_n = (\boldsymbol{\varphi}_1, \ldots \boldsymbol{\varphi}_{20})$ and $\mathbf{a}(t) = (a_1(t), \ldots, a_{20}(t))^T$.

D. Construction of the model for the first n=20 POD coefficients

In order to derive the model for the POD coefficients the Galerkin Projection was used. If we define a residual function $R(\mathbf{x}, \dot{\mathbf{x}})$ for equation (2) as follows:

$$R(\mathbf{x}, \dot{\mathbf{x}}) = \dot{\mathbf{x}}(t) - \mathbf{A}\mathbf{x}(t) - \mathbf{B}\mathbf{u}(t) - \mathbf{F}\mathbf{d}(t) \tag{7}$$

and we replace $\mathbf{x}(t)$ by its nth order approximation $\mathbf{x}_n(t)$ in (7), the Galerkin projection states that the projection of $R(\mathbf{x}_n, \dot{\mathbf{x}}_n)$ on the space spanned by the basis vectors $\boldsymbol{\Phi}_n$ vanishes. That is,

$$\left\langle R(\mathbf{x}_n, \dot{\mathbf{x}}_n), \boldsymbol{\varphi}_j \right\rangle = 0; \quad j = 1, \ldots n \tag{8}$$

where $\langle ., . \rangle$ denotes inner product. Replacing $\mathbf{x}(t)$ by its nth order approximation $\mathbf{x}_n(t) = \boldsymbol{\Phi}_n\mathbf{a}(t)$ in equation (2), and applying the inner product criterion (Galerkin projection) to the resulting equation we have:

$$\langle \boldsymbol{\Phi}_n\dot{\mathbf{a}}(t), \boldsymbol{\Phi}_n \rangle = \langle \mathbf{A}\boldsymbol{\Phi}_n\mathbf{a}(t) + \mathbf{B}\mathbf{u}(t) + \mathbf{F}\mathbf{d}(t), \boldsymbol{\Phi}_n \rangle . \tag{9}$$

By evaluating the inner product in (9), we obtain the model for the first n time varying coefficients and therefore the reduced order model of the reactor with only 20 states,

$$\begin{aligned} \dot{\mathbf{a}}(t) &= \mathbf{A}_{\text{r}}\mathbf{a}(t) + \mathbf{B}_{\text{r}}\mathbf{u}(t) + \mathbf{F}_{\text{r}}\mathbf{d}(t) \\ \mathbf{x}_n(t) &= \boldsymbol{\Phi}_n\mathbf{a}(t) \end{aligned} \tag{10}$$

where $\mathbf{A}_{\text{r}} = \boldsymbol{\Phi}_n^T\mathbf{A}\boldsymbol{\Phi}_n$, $\mathbf{B}_{\text{r}} = \boldsymbol{\Phi}_n^T\mathbf{B}$ and $\mathbf{F}_{\text{r}} = \boldsymbol{\Phi}_n^T\mathbf{F}$.

The discrete-time version of (10) that is used by the digital controller, was obtained using the bilinear transformation with a sampling time of $0.2s$,

$$\begin{aligned} \mathbf{a}(k+1) &= \tilde{\mathbf{A}}\mathbf{a}(k) + \tilde{\mathbf{B}}\mathbf{u}(k) + \tilde{\mathbf{F}}\mathbf{d}(k) \\ \mathbf{x}_n(k) &= \boldsymbol{\Phi}_n\mathbf{a}(k) \end{aligned} \tag{11}$$

where $\tilde{\mathbf{A}}$, $\tilde{\mathbf{B}}$ and $\tilde{\mathbf{F}}$ are the matrices describing the new system. The sampling time was chosen by dividing the faster time constant of the system (10) by 10.

IV. CONTROL SCHEMES

The control goal is to reject the disturbances that affect the reactor, that is the changes in the temperature and concentration of the feeding flow. Additionally the control actions must satisfy the inputs constraints of the process and the control system must keep the temperature inside the reactor below 400 K. In the following subsections two MPC control schemes will be presented, the scheme proposed in [1] and a new control scheme. The simulation results will be discussed as well.

TABLE I

PERFORMANCE PARAMETERS OF THE CONTROL SYSTEMS

Control	Test 1		Test 2		Test 3		Test 4	
	$T_{\max}$ [K]	$\Delta C_{\text{out}}[\%]$	$T_{\max}$ [K]	$\Delta C_{\text{out}}[\%]$	$T_{\max}$ [K]	$\Delta C_{\text{out}}[\%]$	$T_{\max}$ [K]	$\Delta C_{\text{out}}[\%]$
Open-Loop	413.03	-79.39	390	198.25	441.4	-99.57	390	493.7
MPC-S1	394.09	-0.69	397.59	3.19	407.1	56.82	399.67	134
MPC-S2	394.59	-0.7	395.05	0.63	398.63	-9.073	399.34	-54.12

A. First MPC control scheme (MPC-S1)

In the MPC control system proposed in [1], the control of the temperature and concentration profiles is achieved indirectly by controlling the POD coefficients. The references ($\mathbf{a}_{\text{ref}}$) of the POD coefficients were found by means of the following formula:

$$\mathbf{a}_{\text{ref}} = \mathbf{\Phi}_n^T \mathbf{x}_{\text{ref}} \tag{12}$$

where $\mathbf{x}_{\text{ref}}$ is the reference of the vector $\mathbf{x}(t)$ and is equal to $\mathbf{0}$ since the control system has to keep the reactor operating around the profiles shown in Figure 2. The formulation of the MPC Controller is as follows:

$$\min_{a,\Delta u} J = \sum_{k=1}^{N_{\text{p}}} \|\mathbf{a}_{\text{ref}}(k) - \mathbf{a}(k)\|_{\mathbf{Q}}^2 + \sum_{k=0}^{N_{\text{c}}-1} \|\Delta \mathbf{u}(k)\|_{\mathbf{R}}^2 \tag{13}$$

subject to

$$\mathbf{a}(k+1) = \tilde{\mathbf{A}}\mathbf{a}(k) + \tilde{\mathbf{B}}\mathbf{u}(k) + \tilde{\mathbf{F}}\mathbf{d}(k)$$

$$\mathbf{d}(k+1) = \mathbf{d}(k), \quad \mathbf{u}_{\min} \leq \mathbf{u}(k) \leq \mathbf{u}_{\max}$$

where $\|\mathbf{v}\|_{\mathbf{Q}}^2$ denotes $\mathbf{v}^T\mathbf{Q}\mathbf{v}$, $\Delta\mathbf{u}(k) = \mathbf{u}(k) - \mathbf{u}(k-1)$, N_{p} is the prediction horizon, N_{c} is the control horizon, $\mathbf{Q}$ and $\mathbf{R}$ are weighting matrices, and $\mathbf{u}_{\min}$ and $\mathbf{u}_{\max}$ are the lower and upper bounds of $\mathbf{u}(k)$. It is important to remark that the temperature constraint ($T(z,t) \leq 400$ K) of the reactor has not been included in this MPC formulation.

Given that the state vector $\mathbf{a}(k)$ is unknown and the changes in the concentration of the feeding flow ($d_1(k) = \bar{C}_{\text{in}}^{\Delta}(k)$) are not measured directly, they are estimated by means of an observer (in this case a Kalman Filter) with the following formulation:

$$\begin{pmatrix} \hat{\mathbf{a}}(k+1) \\ \hat{d}_1(k+1) \end{pmatrix} = \begin{pmatrix} \tilde{\mathbf{A}} & \tilde{\mathbf{F}}_{\text{C}} \\ \mathbf{0} & 1 \end{pmatrix} \begin{pmatrix} \hat{\mathbf{a}}(k) \\ \hat{d}_1(k) \end{pmatrix} + \begin{pmatrix} \tilde{\mathbf{B}} \\ \mathbf{0} \end{pmatrix} \mathbf{u}(k)$$

$$+ \begin{pmatrix} \tilde{\mathbf{F}}_{\text{T}} \\ 0 \end{pmatrix} d_2(k) + \begin{pmatrix} \mathbf{L}_{\text{a}} \\ \mathbf{L}_{\text{d}} \end{pmatrix} (\mathbf{y}(k) - \hat{\mathbf{y}}(k)) \tag{14}$$

$$\hat{\mathbf{y}}(k) = \mathbf{C}_{\text{s}}\hat{\mathbf{x}}_n(k) = \mathbf{C}_{\text{s}}\mathbf{\Phi}_n\hat{\mathbf{a}}(k)$$

where $\hat{\mathbf{a}}(k)$ is the estimated vector of the POD coefficients, $\hat{d}_1(k)$ is the estimation of $\bar{C}_{\text{in}}^{\Delta}(k)$, $d_2(k)$ is the normalized temperature deviations of the feeding flow ($\bar{T}_{\text{in}}^{\Delta}(k)$), $\mathbf{y}(k) \in \Re^4$ is a vector which contains the temperature measurements (normalized deviations) along the reactor, $\hat{\mathbf{y}}(k)$ is the estimation of $\mathbf{y}(k)$, $\mathbf{L}_{\text{a}}$ and $\mathbf{L}_{\text{d}}$ are the submatrices of the observer gain (Kalman gain), $\tilde{\mathbf{F}}_{\text{C}}$ and $\tilde{\mathbf{F}}_{\text{T}}$ are the column vectors of $\tilde{\mathbf{F}} = (\tilde{\mathbf{F}}_{\text{C}}, \tilde{\mathbf{F}}_{\text{T}})$ and $\mathbf{C}_{\text{s}}$ is a selection matrix which selects the measured temperatures from the vector $\mathbf{x}_n(k)$.

The control horizon N_{c} was set to 10 samples and the prediction horizon N_{p} was selected according to the following criterion: "Prediction Horizon = Control Horizon + Largest Settling Time = 80 samples". $\mathbf{u}_{\min}$ and $\mathbf{u}_{\max}$ were selected according to the input constraints of the process and the operating temperatures of the jackets, and the weighting matrices in this way: $\mathbf{Q} = \mathbf{I}_{20\times 20}$, $\mathbf{R} = 110 \cdot \mathbf{I}_{3\times 3}$.

B. Second MPC control scheme (MPC-S2)

Unlike the previous control system, in this scheme the formulation of the MPC controller is in terms of physical variables. These variables are the temperature of some selected points along the reactor and the concentration at the reactor outlet. This formulation makes the tuning procedure more intuitive and allows us to have more flexibility in the definition of the control objectives; we can give more importance to the concentration at the reactor outlet with respect to the temperature of the selected points or vice versa. In this MPC formulation, the temperature constraint ($T(z,t) \leq 400$ K) of the system is imposed in the selected points. It has been observed through simulations that only imposing the temperature constraint in some points, is sufficient for guaranteeing the satisfaction of the temperature constraint in the remaining points of the spatial domain.

Since in this MPC formulation the temperature constraint along the reactor is taken into account, it is necessary to use a mechanism for handling the infeasibilities that can emerge due to the differences between the process and the model used by the MPC, the magnitude of the disturbances, the saturation of the actuators, etc. A way to deal with these infeasibilities is by softening the temperature constraint through a slack variables approach. A soft constraint formulation avoids infeasibilities problems by allowing violations in the temperature (output) constraint, but at the same time it tries to minimize such violations by penalizing them in the objective function. In this paper a slack variable approach with ℓ_∞-norm and time-dependent weights is used [7]. The formulation of the MPC controller is as follows:

$$\min_{a,\Delta u,\varepsilon} J = \sum_{k=1}^{N_{\text{p}}} \left(\left\| \bar{\mathbf{T}}_{\text{p,ref}}^{\Delta}(k) - \bar{\mathbf{T}}_{\text{p}}^{\Delta}(k) \right\|_{\mathbf{Q}_{\text{T}}}^2 + \right. \tag{15}$$

$$\left. + \left\| \bar{C}_{N,\text{ref}}^{\Delta}(k) - \bar{C}_{N}^{\Delta}(k) \right\|_{Q_{\text{C}}}^2 \right) + \sum_{k=0}^{Nc-1} \|\Delta \mathbf{u}(k)\|_{\mathbf{R}}^2 + \mathbf{P}^{\mathbf{T}}\boldsymbol{\varepsilon}$$

subject to

$$\mathbf{a}(k+1) = \tilde{\mathbf{A}}\mathbf{a}(k) + \tilde{\mathbf{B}}\mathbf{u}(k) + \tilde{\mathbf{F}}\mathbf{d}(k), \;\; \mathbf{x}_n(k) = \mathbf{\Phi}_n\mathbf{a}(k)$$

$$\mathbf{d}(k+1) = \mathbf{d}(k), \quad \mathbf{u}_{\min} \leq \mathbf{u}(k) \leq \mathbf{u}_{\max}$$

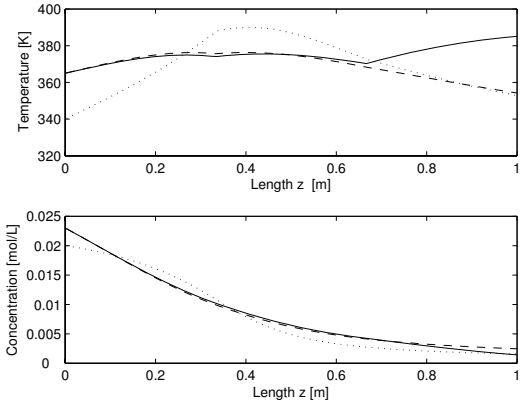

Fig. 3. Steady-State Temperature and Concentration profiles for test 3. Dotted line- Nominal profile. Dashed Line- MPC-S1. Solid Line- MPC-S2.

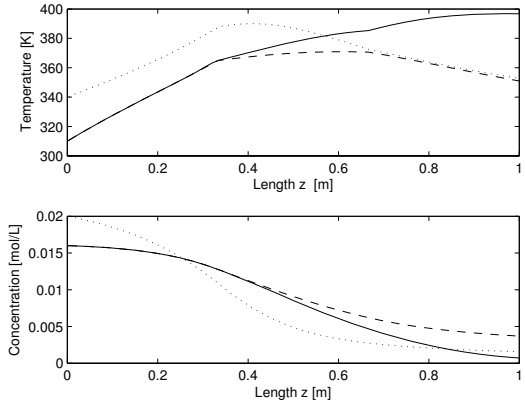

Fig. 4. Steady-State Temperature and Concentration profiles for test 4. Dotted line- Nominal profile. Dashed Line- MPC-S1. Solid Line- MPC-S2.

$$\bar{\mathbf{T}}_{\mathrm{p}}^{\Delta}(k) \leq \bar{\mathbf{T}}_{\mathrm{p}}^{\Delta_{\max}} + \eta(k)\boldsymbol{\varepsilon}, \quad \boldsymbol{\varepsilon} \geq 0$$

where $\|\mathbf{v}\|_{\mathbf{Q}}^2$ denotes $\mathbf{v}^T\mathbf{Q}\mathbf{v}$, $\bar{\mathbf{T}}_{\mathrm{p}}^{\Delta}(k)$ is a vector which contains the normalized deviations of the temperature of the selected points, $\bar{C}_N^{\Delta}(k)$ is the normalized deviation of the concentration at the reactor outlet, $\bar{\mathbf{T}}_{\mathrm{p,ref}}^{\Delta}(k)$ and $\bar{C}_{N,\mathrm{ref}}^{\Delta}(k)$ are the references for $\bar{\mathbf{T}}_{\mathrm{p}}^{\Delta}(k)$ and $\bar{C}_N^{\Delta}(k)$ respectively, $\Delta\mathbf{u}(k) = \mathbf{u}(k) - \mathbf{u}(k-1)$, $\mathbf{Q}_{\mathrm{T}}$ and $\mathbf{R}$ are weighting matrices, Q_{C} is a weighting factor, $\mathbf{P}$ is a weighting vector, N_{p} is the prediction horizon, N_{c} is the control horizon, $\mathbf{u}_{\min}$ and $\mathbf{u}_{\max}$ are the lower and upper bounds of $\mathbf{u}(k)$, $\bar{\mathbf{T}}_{\mathrm{p}}^{\Delta_{\max}}$ is a vector which contains the maximum allowed temperatures for the selected points, $\boldsymbol{\varepsilon} \in \Re^{20}$ is the vector of the slack variables, and $\eta(k) = 1/r^{k-1}$, is a time-dependent weight ($r > 1$).

For estimating the state vector $\mathbf{a}(k)$ and the changes in the concentration of the feeding flow ($d_1(k) = \bar{C}_{\mathrm{in}}^{\Delta}(k)$), the same observer used by the first control scheme was used (see equation (14)). The points where the temperature is controlled were found by trial and error. Seven points were used and they correspond to the following sections of the reactor ($N = 300$ sections): 100, 122, 150, 200, 250, 270, 300. The parameters of the MPC controller were set as follows: $N_{\mathrm{c}} = 10$ samples, $N_{\mathrm{p}} = 80$ samples, $r = 1.2$, $\mathbf{P} \in \Re^7 = 10^4 \cdot (1, 1, \ldots, 1)^T$, $\mathbf{Q}_{\mathrm{T}} = \mathbf{I}_{7\times 7}$, $Q_{\mathrm{C}} = 1000$, $\mathbf{R} = 110 \cdot \mathbf{I}_{3\times 3}$. The references for the variables were selected in this way: $\bar{\mathbf{T}}_{\mathrm{p,ref}}^{\Delta} = \mathbf{0}$, and $\bar{C}_{N,\mathrm{ref}}^{\Delta} = -5 \cdot 10^{-3}$ (reduction of 6.5%). Notice that in this tuning, it is considered more important to bring the concentration at the reactor outlet to its desired value than to bring the temperatures of the selected points to their references.

C. Simulation Results

Initially in order to evaluate the performance of the control systems the following tests were carried out:

- Test 1: the temperature and concentration of the feeding flow are increased in 10 K and 10^{-3} mol/L respectively.
- Test 2: the temperature and concentration of the feeding flow are decreased in 10 K and 10^{-3} mol/L respectively.

For the simulations, the nonlinear model of the process given in (1) was discretized in space by replacing the partial derivatives with respect to space by backward difference approximations [2][8]. In table I, some quantities for quantifying the performance of the control systems are shown. In this table, $T_{\max}$ is the maximum temperature reached inside the reactor during the test. ΔC_{out} is the percentage of change of the concentration in steady state at the reactor output with respect to its nominal value. That is, $\Delta C_{\mathrm{out}}(\%) = 100 \cdot (C_N - C_N^*)/C_N^*$, where C_N^* is the nominal value ($1.5737 \cdot 10^{-3}$ mol/L) and C_N is the concentration in steady state after the test.

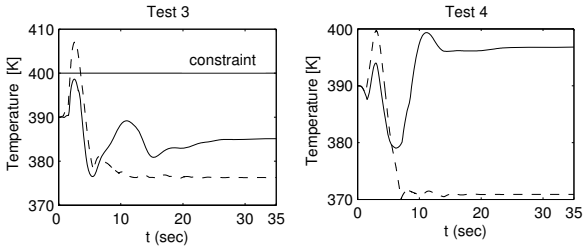

Fig. 5. Maximum peak of the temperature profile. Dashed line- MPC-S1. Solid Line- MPC-S2.

In Test 1, there is a permanent violation of the temperature constraint for the open-loop case. The maximum temperature value registered was 413.03 K, which is far from the maximum allowed (400 K). On the other hand, the MPC control schemes keep the temperature inside the reactor below 400 K and at the same time they reduce a little bit the concentration at the reactor outlet.

In Test 2, a significant increment of the concentration at the reactor outlet is observed when the system is operating in an open-loop configuration. We have an increment of 198.25% in steady state, which means that the performance of the tubular chemical reactor has been reduced dramatically. With the MPC controllers we have an increment in the concentration of only 3.19% for the first controller and 0.63% for the second one. It is clear that the performance of the reactor practically has not been affected.

In the previous tests, the control actions of both MPC control systems were all the time within the allowed boundaries. In general, the control schemes showed a good behavior for rejecting the disturbances and both control systems presented a similar performance.

In order to evaluate the ability of the second control scheme of dealing with the temperature constraint along the reactor, the following tests were designed:

- Test 3: the temperature and concentration of the feeding flow are increased in 25 K and $3 \cdot 10^{-3}$ mol/L respectively.
- Test 4: the temperature and concentration of the feeding flow are decreased in 30 K and $4 \cdot 10^{-3}$ mol/L respectively.

It is important to remark that under these new tests (where the disturbances are too large in comparison with the typical ones) the tubular reactor operates far from the operating profiles shown in Figure 2, and therefore the differences between the nonlinear model of the process and the linear POD model used by the controllers are considerably large.

The simulation results of the Tests 3 and 4 are presented in Figures 3, 4 and 5. Table I shows the performance parameters of the control systems. In Test 3, the first MPC control system violates temporarily the temperature constraint as can be observed in Figure 5. The constraint is violated during $1.66s$ and the maximum peak registered was 407.1 K. On the other hand the second MPC keeps all the time the temperature profile below 400 K. It is important to keep in mind that the first MPC controller does not take into account the temperature constraint and the results obtained with it were expected. From table I, it is clear that the performance of the reactor is degraded in a considerable way (the concentration at the reactor outlet is increased in 56.82%) when the first MPC scheme is used, whereas the performance of the reactor is increased with the second one. Notice in Figure 3, how the last part (particularly when $z > 0.667$ m) of the temperature profiles is different. The temperature profile of the second control scheme is over the profile of the first control system allowing a good reduction of the concentration at the reactor outlet. This behavior is the consequence of giving more weight to the concentration ($Q_{\mathrm{C}} = 1000$) than to the temperature of the selected points ($\mathbf{Q}_{\mathrm{T}} = \mathbf{I}_{7\times 7}$) in the formulation of the second MPC.

In test 4, there is not violation of the temperature constraint (see Figure 5) when both MPC control systems are used. It is remarkable how the second MPC reduces the concentration at the reactor outlet in 54.12%. This is not the case for the first control scheme where the concentration at the reactor outlet is increased in 134%.

In the previous tests, the control actions of both MPC control systems were all the time within the allowed limits. From these tests it is evident that the second control scheme notably outperforms the first one when large disturbances are applied to the reactor. It is remarkable how the second MPC can deal with the temperature constraint of the system in spite of using a linear-POD model of the tubular reactor.

V. CONCLUSIONS

In this paper a new POD-based MPC control scheme for controlling the temperature and concentration profiles of a non-isothermal tubular reactor has been presented. The formulation of the predictive controller is in terms of physical variables, which makes its tuning very intuitive and the definition of the control goals more flexible than in other approaches. The controller also incorporates in its formulation the temperature constraint of the reactor ($T(z,t) \leq 400$ K), and it showed a good behavior in the presence of large disturbances, in spite of it uses a reduced-order linear model of the system. However, it is important to remark that the tuning of the controller has been done in a conservative way. If a tight tuning is required, it would be necessary to incorporate the nonlinear characteristics of the reactor into the POD model. In this paper the selection of the points where the temperature constraint is imposed was done by trial and error. Future research is necessary in order to find a method for selecting those points in such a way that the selection guarantees the satisfaction of the temperature constraint for the remaining points in the spatial domain.

VI. ACKNOWLEDGMENTS

This research was supported by: • Research Council KUL: GOA AMBioRICS, CoE EF/05/006 Optimization in Engineering, several PhD/postdoc & fellow grants; • Flemish Government: ○ FWO: PhD/postdoc grants, projects, G.0407.02 (support vector machines), G.0197.02 (power islands), G.0141.03 (Identification and cryptography), G.0491.03 (control for intensive care glycemia), G.0120.03 (QIT), G.0452.04 (new quantum algorithms), G.0499.04 (Statistics), G.0211.05 (Nonlinear), G.0226.06 (cooperative systems and optimization), G.0321.06 (Tensors), G.0302.07 (SVM/Kernel), research communities (ICCoS, ANMMM, MLDM); ○IWT: PhD Grants, McKnow-E, Eureka-Flite2 • Belgian Federal Science Policy Office: IUAP P6/04 (Dynamical systems, control and optimization, 2007-2011) ; • EU: ERNSI. Dr. Bart De Moor is a full professor at the Katholieke Universiteit Leuven, Belgium.

REFERENCES

[1] O.M. Agudelo, J.J. Espinosa, B. De Moor, "Control of a Tubular Chemical Reactor by means of POD and Predictive Control Techniques", *in Proceedings of the European Control Conference 2007 (ECC 2007)*, pp. 1046-1053, Kos, Greece, 2007.

[2] I.Y. Smets, J.F. Van Impe,"Optimal Control of Tubular Chemical Reactors: Performance Assessment under transient and Diffuse conditions", *in Proceedings of the 10th Mediterranean Conference on Control and Automation - MED2002*, Lisbon, Portugal, 2002.

[3] M. Fjeld and B. Ursin, "Approximate lumped models of a tubular chemical reactor, and their use in feedback and feedforward control", *in Proceedings of the 2nd IFAC Symposium on Multivariable Technical Control Systems*, pp. 1-18, North Holland, Amsterdam, 1971.

[4] P. Astrid, "Reduction of Process Simulation Models: a proper orthogonal decomposition approach", Ph.D. thesis, Technishche Universiteit Eindhoven, Eindhoven, Netherlands, 2004.

[5] L. Huisman,"Control of Glass Melting Processes Based on Reduced CFD models", Ph.D. thesis, Technishche Universiteit Eindhoven, Eindhoven, Netherlands, 2005.

[6] M. Hazenberg, P. Astrid and S. Weiland, "Low order modeling and optimal control design of a heated plate", *in Proceedings of the 5th European Control Conference*, Cambridge, 2003.

[7] M. Hovd, R. D. Braatz, "Handling State and Ouput Constraints in MPC using Time-dependent Weights", *in Proceedings of the American Control Conference*, Arlington, USA, 2001.

[8] D. Del Vecchio and N. Petit, "Boundary Control for an industrial under-actuated tubular chemical reactor", *Journal of Process Control*, vol 15, pp. 771-784, 2005